Exploration of Nonlinear Mixed Convection Williamson Nanoliquid Flow Generated by a Nonlinearly Elongating Sheet in the Neighbourhood of Stagnation-Point

Hammed Fatai Akangbe[1], Akanbi Olumuyiwa Olawale[2]

[1]*Department of Mathematical Sciences, Olabisi Onabanjo University, Ago-Iwoye, Nigeria*
[2]*Department of Mathematics and Statistics, Federal Polytechnic, Ilaro, Nigeria*

Abstract: The present investigation delves into the flow of a magnetized non-Newtonian Williamson fluid by nonlinear mixed convection. A stagnation point regulates the fluid's motion. The mathematical model underlying the problem is transmuted via similarity transformations to exhibit ordinary derivative equations of order three. Consequently, a numerical solution is obtained through the Runge-Kutta-Fehlberg approach in conjunction with the shooting technique. The influences of some dimensionless physical terms such as the magnetic field, Eckert, Schmidt and Prandtl numbers coupled with activation energy are discussed graphically. The numerical results demonstrate a flawless connection when compared to pertinent literature results in limited contexts. The analysis reveals a decrease in velocity profile and a rise in fluid temperature are observed when the magnitude of the viscosity and magnetic field parameters increases. An increase in radiation and heat source parameters leads to an increase in the heat transfer rate, whereas factors involving viscosity and magnetic field slow down the fluids but drive a rise in the temperature distribution. The solutal boundary structure is enhanced due to the escalating nature of activation energy, whereas a diminished trend occurs with the chemical reaction and Schmidt number.

Keywords: Nonlinear mixed convection; Elongating sheet; Williamson nanoliquid; Stagnation-point; Dimensionless parameters.

1. Introduction

The non-Newtonian fluids have innumerable uses in a wide range of human undertakings; hence, their studies are gaining much interest from scientists and researchers. This class of fluid is common in the oil drilling industry, paints rheology, molten polymers, mud drilling, the drug and pharmaceutical industry, the cosmetics industry, etc. Several authors have reported on the importance of non-Newtonian fluids in industrial and engineering works [1-2]. Highly nonlinear and complex equations are required to describe the flow of non-Newtonian fluids, which differ significantly from the flow of Newtonian fluids due to the stress tensors' nonlinear relation to the deformation rate. Since no single constitutive model can fully account for the properties of these fluids, various theories and concepts have been developed to try and capture their flow characteristics. Some of the many fluid models used to describe non-Newtonian fluids are the Williamson fluid, the Carreau fluid, the Jeffery fluid, the Maxwell fluid, the micropolar fluid, and the Giesekus fluid [3-5].

The Williamson fluid model stands out among the rest. For example, as shear stress rates increase, the fluid's viscosity thins, demonstrating its non-Newtonian fluid nature. This class of fluids includes plasma blood and emulsion sheets like those used in photography. Nadeem et al. [6] were the first to develop the boundary layer transport of such fluids along a stretched surface, building on the work of Williamson [7]. This has led to a plethora of studies that consider various aspects, such as the geometry of the flow, heating conditions at the energy field, etc. In the investigation of the Williamson fluid on Blasius flow near a stagnation point, Sha et al. [8] evaluated the significance of heat transmission in the presence of thermal radiation over the permeable elongated device. Quran et al. [9] evaluated how Williamson fluid is affected by forced convection forces and uniform heat transmission at the boundary using a numerical procedure on a porous material medium. The results showed that the Williamson fluid has the tendency to increase the shear stress and the velocity profiles.

Flowing fluids across extending plates are often encountered in diverse areas of industry and technology. Many potential applications are found in the production of polymers, extrusion of plastic sheets, paper manufacturing, cooling of metal sheets and so on [10-14]. Such investigation evolved from the study of Crane [15]. The author reiterated the possibility of a closed-form solution to a time-independent two-dimensional problem when the sheet extended in a linear form. Other researchers have discussed the possibility of a nonlinear elongating sheet (see Refs [16-17], which is more realistic in practical situations such as wire drawing.

The present study deals with Williamson fluid flowing across a nonlinearly extending sheet due to real engineering applications.

Fluids composed of nanoparticles (small particles) of metals, oxides, etc., are called nanofluids [18-19]. Researchers have reported an enhanced thermal conductivity when this new fluid category is used compared to traditional base fluids (such as water, oil, ethylene glycol, etc.). Many engineering and industrial processes rely on heating and cooling fluids, such as power production and atomic reactors; as such, the cooling process becomes vital in high-energy equipment in such fields. Due to its potential usefulness in a wide range of fields relevant to modern society, including medicine, transportation, and electronics, nanofluid research has recently gained much scholarly attention [20-22].

The present study aims to examine the impact of several critical parameters on the flow of a reactive magnetised Williamson nanofluid in the presence of nonlinear mixed convection, activation energy, thermal radiation, thermo-migration of small particles, Brownian motion of the particles, and convective heating of the thermal boundary layer. The thermal conductivity and an external heat source cause a nonlinearly expanding plate to undergo the motion. The study has important implications for chemical and extrusion operations. A numerical solution is employed to discuss the parametric effects of crucial terms on the non-dimensional velocity, temperature, and concentration profiles.

2. Development of the Problem

As illustrated in Figure 1. A Williamson nanoliquid is flowing across a two-dimensional extending material device in the neighbourhood a stagnation point. It is assumed that the fluid motion is time-independent; it is simply laminar and not turbulent, and it is not compressible as well. The extending plate causes the flow and that the device stretches in a nonlinear fashion with the surface velocity $u_w = bx^m$ at the wall and velocity $U_e = ax^m$ at the far field. A convective heating type is adhered to in the thermal region, but the ambient temperature relates to that of the fluid. The coordinates of the material device are described using (x, y) and their respective velocity components are (u, v). The radiative heat flux is simplified by Rosseland approximation, there is an internal heat generation in the energy field while the nanoparticles concentration field consists of the chemical reaction in conjunction with the activation energy. The application of non-uniform external magnetic field $B(x)\left(B(x) = B_0 x^{\left(\frac{m}{2}-\frac{1}{2}\right)}\right)$ on the direction of flow is done on the material device but no account of the induced magnetic field is considered. The thermophysical attributes of the fluid are functions of temperature.
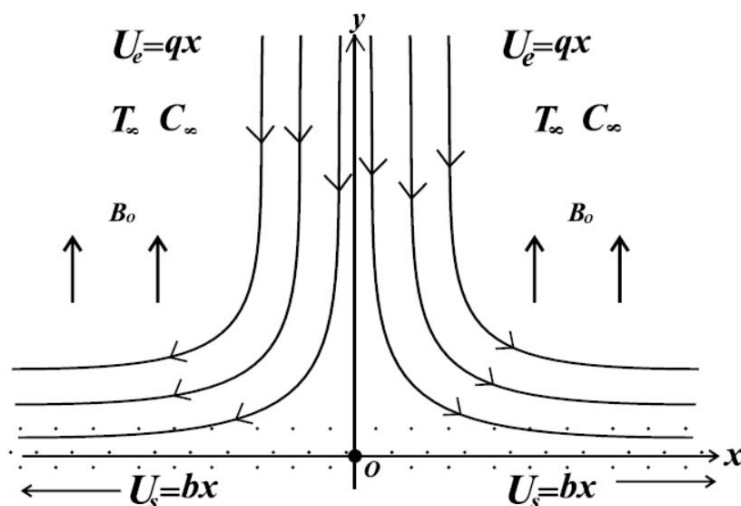

Figure 1 Sketch of the configuration

On the basis of the aforementioned assumptions, the transport equations are listed as follows

$$\frac{\partial U}{\partial x} + \frac{\partial V}{\partial y} = 0, \tag{1}$$

$$U\frac{\partial U}{\partial x} + V\frac{\partial V}{\partial y} - U_e\frac{dU_e}{dx} = \frac{\mu}{\rho_f}\frac{\partial^2 U}{\partial y^2}\left(1 + \sqrt{2}\Gamma\frac{\partial U}{\partial y}\right) + g\left[\beta_1\left(T - T_\infty\right) + \beta_2\left(T - T_\infty\right)^2\right] +$$
$$g\left(G - G_\infty\right) - \frac{\sigma}{\rho_f}(B(x))^2(U - U_e). \tag{2}$$

$$U\frac{\partial T}{\partial x} + V\frac{\partial T}{\partial y} = \frac{1}{(\rho c_p)_f}\frac{\partial}{\partial y}\left(k\frac{\partial T}{\partial y}\right) + \gamma\left[\frac{D_T}{T_\infty}\left(\frac{\partial T}{\partial y}\right)^2 + D_B\left(\frac{\partial T}{\partial y}\frac{\partial C}{\partial y}\right)\right] + \frac{Q(x)\left(T - T_\infty\right)}{(\rho c_p)_f} +$$
$$\frac{\mu}{(\rho c_p)_f}\left[\left(\frac{\partial u}{\partial y}\right)^2 + \Gamma\left(\frac{\partial U}{\partial y}\right)^3\right] + \frac{16\sigma^\star}{3\beta_\star(\rho c_p)_f}\frac{\partial}{\partial y}\left(T^3\frac{\partial T}{\partial y}\right) + \frac{\sigma}{(\rho c_p)_f}B((x))^2(U - U_e)^2, \tag{3}$$

$$U\frac{\partial G}{\partial x} + v\frac{\partial G}{\partial y} = D_B\frac{\partial C^2}{\partial y^2} + \frac{D_T}{T_\infty}\left(\frac{\partial^2 T}{\partial y^2}\right) - k_1^2\left(G - G_\infty\right)\left(\frac{T}{T_\infty}\right)^a \exp\left(-\frac{E_e}{\lambda T}\right). \tag{4}$$

The boundary constraints are listed as:

$$U(x,y) = U = bx^m, V(x,0) = 0, -k_\infty\frac{\partial T}{\partial y} = -g_b\left(T_\infty - T_f\right), G(x,y) = G_w \text{ at } y = 0$$
$$u \to U_e = ax^m, T \to T_\infty, G \to G_\infty, \text{as } y \to \infty. \tag{5}$$

These symbols that are included in the governing equations are u, v which is a component of velocity in x, y directions, T indicating Temperature, v∞ meaning ambient kinematic viscosity, G denoting nanoparticles concentration, ρ_∞which is ambient fluid density, $U_e$indicating far field velocity, μ_∞ meaning a ambient Fluid viscosity, $U_w$connoting surface velocity σ standing for electrical conductivity, $h_T$connoting coefficient of heat transfer, h1 symbolizing chemical reaction rate, $h_c$is the mass transfer coefficient, Γ standing for the relaxation time, T_∞indicating the far field temperature, (ρf) connoting nanofluid density, C_∞indicating far field concentration. Similarly, (ρ_p) stands for nanoparticles density but E_0means activation energy while $(\rho c_p)_f$indicates heat capacity of nanoparticles whereas $(\rho c_p)_f$shows the heat capacity of the fluid. More so, $D_B$represents coefficient of Brownian motion, $D_T$indicates thermophoretic diffusion coefficient, $T_f$is standing for surface temperature, G_w is symbolizing sheet concentration, and k stands for thermal conductivity.

Equations (7-9) are the result of plugging in the quantities from Eq. (6) in order to change the governing equations to their ordinary derivatives of order three. Using (6) also satisfies the equation of mass conservation (1).

$$\eta = y\left(\frac{bx^{r-1}}{\nu_\infty}\right)^{1/2}, \psi = \left(\nu_\infty bx^{m+1}\right)^{1/2}f(\eta), \theta(\eta) = \frac{T - T_\infty}{T_f - T_\infty}, \phi(\eta) = \frac{G - G_\infty}{G_w - G_\infty}, k = k_\infty\left(1 + \alpha\theta\right). \tag{6}$$

$$(1 + We f'') f''' + ff'' - \left(\frac{2m}{m+1}\right)f'^2 + mK^2 - \left(\frac{2}{m+1}\right)M\left(f' - K\right) + \lambda_1\theta\left(1 + \lambda_2\theta\right) + \lambda_3\phi = 0, \tag{7}$$

$$(1 + \alpha\theta + Nr)\theta'' + \alpha\theta'^2 + \left(\frac{m+1}{2}\right)Prf\theta' + PrEc\left(1 + \frac{We}{\sqrt{2}}f''\right)f''^2 + Pr(N_t\theta'^2 + N_b\theta'\phi') +$$
$$PrQ\theta + PrEcM\left(f' - K\right)^2 = 0, \tag{8}$$

$$\phi'' + \frac{N_t}{N_b}\theta'' + \left(\frac{m+1}{2}\right)Scf\phi' - Sc\gamma_1\left(1 + \beta\theta\right)^a \exp\left(-\frac{E}{1 + \beta\theta}\right)\phi = 0, \tag{9}$$

In the same vein, the wall constraints are transformed as follows

$$f'(\eta) = 1, f(\eta) = 0, 0'(\eta) = -\zeta(1 - \theta(0)), \phi(\eta) = 1 \ at \ \eta = 0$$
$$f'(\eta) = H, \theta(\eta) = 0, \phi(\eta) = 0 \ as \ \eta \to 0. \tag{10}$$

$$Pr = \frac{\mu_\infty c_p}{k_\infty}, M = \frac{\sigma B_0^2}{b\rho}, Nr = \frac{16\sigma^\star T_\infty^3}{3k^\star k_\infty}, Q = \frac{Q_0(T_w - T_\infty)}{c\rho C_p(T_f - T_\infty)}, Re = \frac{U_s x}{\nu_\infty}, \beta = \frac{(C_f - C_\infty)}{C_\infty}$$

$$Ec = \frac{U_w^2}{C_p(T_w - T_\infty)}, Sc = \frac{\nu_\infty}{D_B}, \gamma_1 = \frac{k_2^2}{b}, E = \frac{E_e}{\lambda T_\infty}, \zeta = \frac{h_f}{k_\infty}\sqrt{\frac{\nu_\infty}{b}}, We = \Gamma\sqrt{2\frac{c^3 x^{3r-1}}{\nu_\infty}}, \tag{11}$$

$$Nb = \frac{(\rho c_p)_p D_B (G_w - G_\infty)}{(\rho c_p)_f \nu}, Nt = \frac{(\rho c_p)_p D_T (T_w - T_\infty)}{(\rho c_p)_f T_\infty \nu}, \gamma = \frac{(\rho c)_p}{(\rho c)_f}, H = \frac{c}{b}.$$

The emerging physical terms listed in equation (11) are described as follows: Ecdenotes Eckert number, Nr indicates radiation term, We indicates Weissenberg number while K defines the stretching ratio, γ1 denotes the chemical reaction term, ϵ shows the thermal conductivity term, E symbolizes the activation energy, β is the temperature relative parameter, M shows the magnetic, δ is the concentration relative parameter, Ntis the thermo-migration term while Nb describes the haphazard motion of the minute particles, whereas Sc(Pr(defines the Schmidt Prandtl) number. For the engineering application of the current work, those quantities of delight are described as (i) the skin frictional factor C_{fx}(ii) the Nusselt number $Nu_x$and (iii) the Sherwood number Sh_xwhich are respectively expressed as

$$C_{fx} = \frac{2\tau_w}{\rho_\infty U_s^2}, Nu_x = \frac{xq_w}{k_\infty(T_f - T_\infty)}, Sh_x = \frac{xq_m}{D_B(C_w - C_\infty)}, \tag{12}$$

The dimensionless forms of these quantities are expressed as:

$$C_{fx}^\star = \frac{1}{2}Re^{\frac{1}{2}}C_{fx} = \left(f''(0) + \frac{We}{2}f''^2(0)\right), \tag{13}$$

And

$$Nu_x^\star = Re_x^{-\frac{1}{2}}Nu_x = -(1 + Nr)\theta'(0), Sh_x^\star = Re_x^{-\frac{1}{2}}Sh_x = -\phi'(0). \tag{14}$$

$$Where \ \tau_w = \mu_\infty\left[\frac{\partial u}{\partial y} + \frac{\Gamma}{\sqrt{2}}\left(\frac{\partial u}{\partial y}\right)^2\right]_{y=0}, q_w = -\left[\left(k_\infty + \frac{16T^3\sigma^\star}{3k^\star}\right)\frac{\partial T}{\partial y}\right]_{y=0}, q_m = -\left(D_B\frac{\partial C}{\partial y}\right)_{y=0}.$$

3. Numerical Method with Validation

For the system of equations (7-9) and its wall constraints expressed in equation (10), we have employed a numerical means to obtain the required solution because the set of equations (7-9) has a grater dimension of nonlinearity nature. The Runge-Kutta-Gills technique has been applied having step size $\nabla_\eta= 0.01$ with absolute tolerance of 10^5. The program had been implemented on Maple 16. The results have been authenticated by comparing the computational data of f″(0) for alterations in M with some published data under restrictive conditions as displayed in Table 2. There are excellent agreement between the current work and those of published records.

Table 2: Computed data for f″(0) for variation in M

M	Mabood et al. [23]	Present results
0	1.000005	1.00000
1	-1.4142143	-1.41421
5	-2.4494893	-2.44949
10	-3.3166242	-3.31662
50	-7.1414285	-7.14143
100	-10.049876	-10.0499

4. Outcomes of the analysis and deliberation

In what follows in this section, we have included several graphs to explain the impact of the emerging terms on the profiles of the dimensionless quantities of interest. Important parameter effects affecting the velocity field and temperature region have been publicized in Figures 2 and 3. In figure 2, there is an exhibition of the character of the magnetic field parameter M as it affects the trend of the velocity. As M increases, flow is

stifled because the transverse magnetic field exerts a Lorentz force on the electrically conducting Williamson fluid, causing resistance to its motion. The flow of the fluid is slowed because when M increases, the Lorentz force also increases, and vice versa. In view of that, there is a thinning of the hydrodynamic bounding structure.
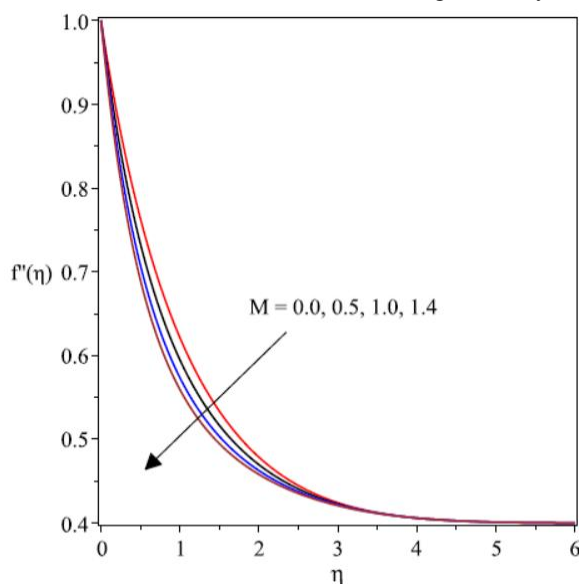

Figure 2 Alterations in velocity field due to changes in M

Different from this, temperature field becomes energized due to friction as a result of growth in M (see Figure 3). Here, the interaction of the Lorentz force and the electric nature of the Williamson fluid prevents the motion of the fluid due to a magnetic field M and in consequence, there is an upsurge in friction, which enables a rise in the heat profiles and thus causes temperature to appreciate, and the thermal boundary structure expands significantly as M grows in magnitude. In this view, the flow and thermal distribution can be modified appropriately by the alterations of the magnetic field term in the flow region.
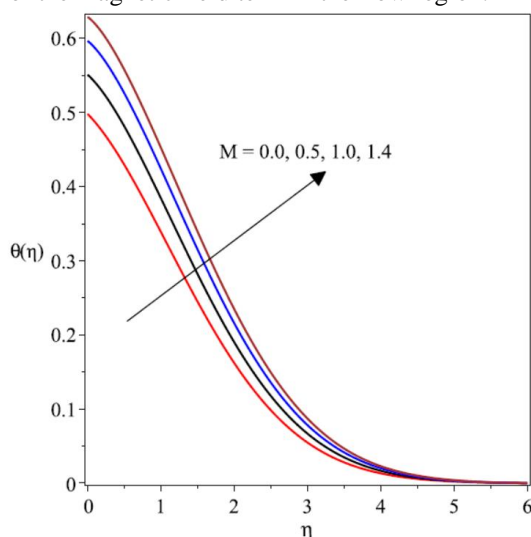
Figure 3 Trend of temperature profiles due to alterations in M

Transport phenomena for the heat and motion profiles owing to changes in the Ec's magnitude are depicted in Figures 4 and 5. Elevated Ec values are associated with an upward shift in the velocity profiles. The thermal neighborhood also increases in value dramatically with increasing Ec. As Ec increases, more heat is generated in the flow field because of the frictional impact of the Williamson fluid particles and the growing sheet. In fact, the thermal bounding surface is seen to enlarge noticeably with increasing Ec.
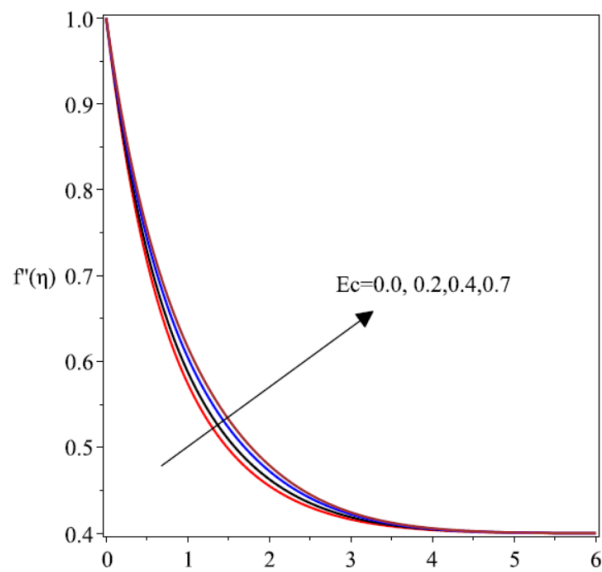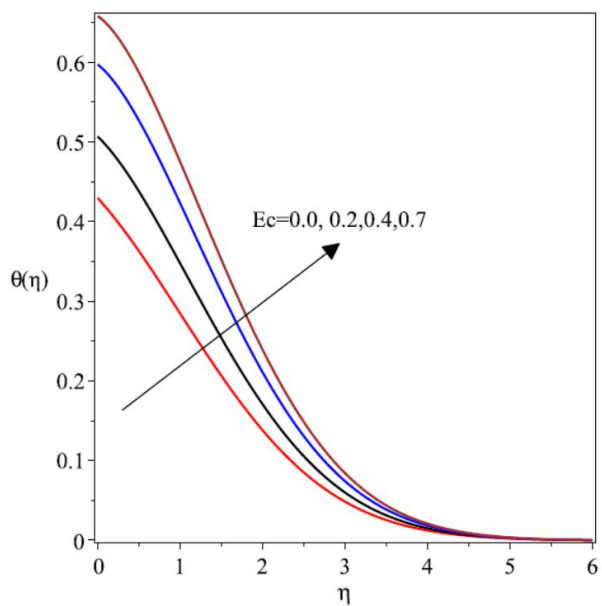
Figure 4 Trend of velocity field as Ec alters

Figure 5 characteristics of temperature profile due to alterations in Ec

The behavioural pattern of the velocity field and that of the thermal region are clearly manifest in figures 6 and 7 due to Pr. As is known, Pr is a description of the thickness of the momentum layer compared to that of the thermal layer.
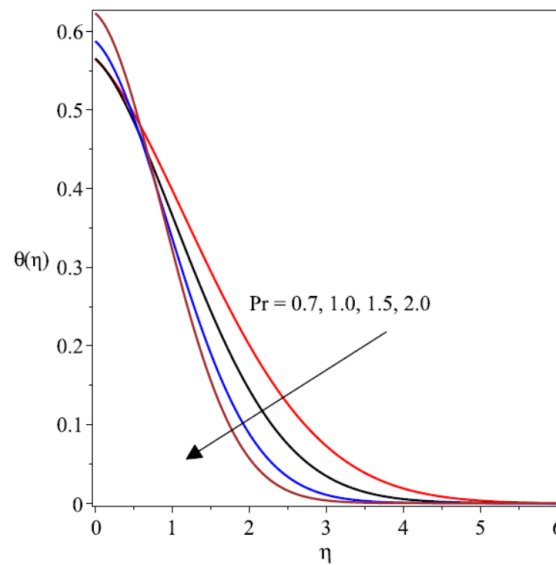
Figure 7 Trend of temperature owing to changes in Pr.

The velocity profiles fall due to Pr because there is a direct relationship between Pr and Williamson fluid viscosity, and so growth in Pr corresponds to higher viscosity, which then creates resistance to the fluid speed. At the same time, the thermal bounding structure thins out as Pr magnifies, and as such, there is a cooling effect as the surface temperature falls significantly.
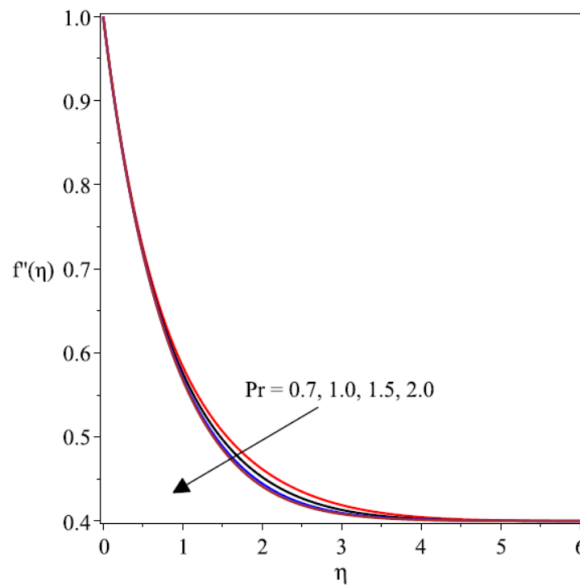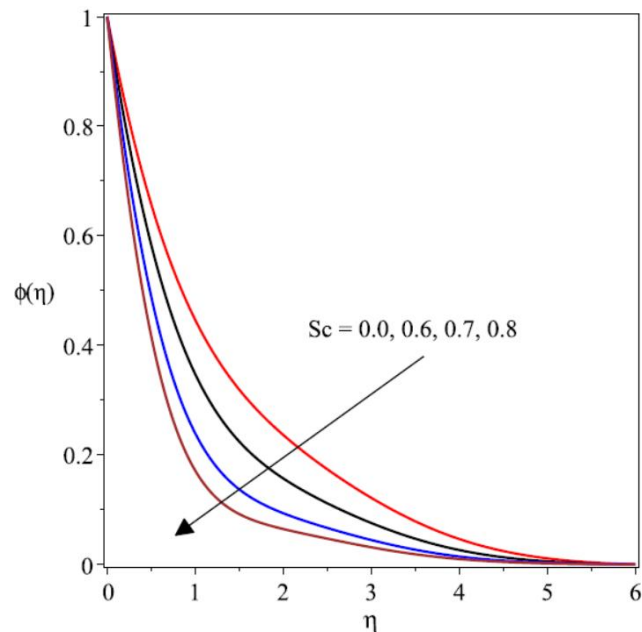

Figure 6 Plot of the velocity field due to alterations in Pr

Figure 8 Trend of the concentration profiles due to Sc

The concentration of nanoparticles is shown to decline in nature as Sc improves in magnitude, as depicted in figure 8. It is known that Sc is a description of the thickness of the momentum layer compared to that of the concentration layer. In this view, a rise in Sc causes the mass diffusivity to drop, and as such, there is a reduction in the concentration bounding surface, as revealed in figure 8. Meanwhile, figure 9 manifests the trend of the concentration profiles versus η as the chemical reaction term changes in value. The concentration of the tiny particles is a decreasing function of γ_1, as found in figure 9. A rise in activation energy parameter boosts the growth of the concentration profiles, as exemplified in figure 10. As is known, E describes the minimum amount of energy required for a reaction process to begin. So, an increase in E energizes the reaction to take place in the concentration region, which led to the expansion of the profiles as portrayed in this figure.
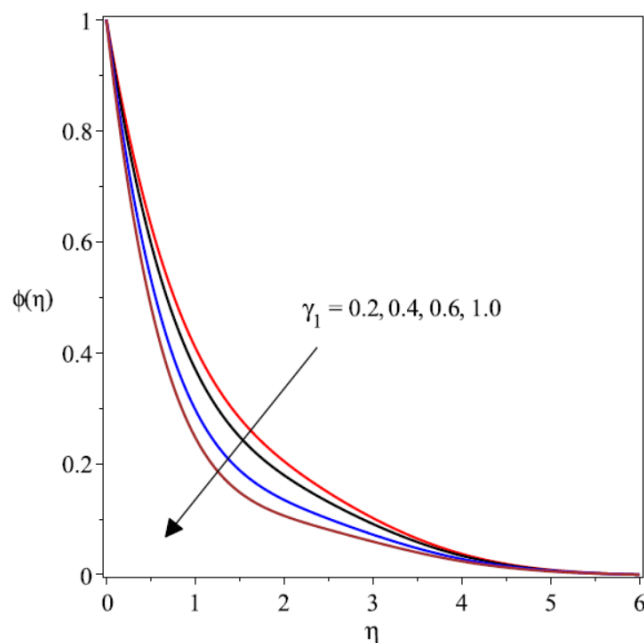

Figure 9 Behaviour of concentration due to alterations in γ_1

The illustration of the thermal and solutal fields due to the alteration in the in Nt is sketched in figures 11 and 12. Clearly, both profiles upsurge due to rising values of Nt. Also, the temperature field field enhances due to the irregular movement of the minute particles Nb as found in figure 13.
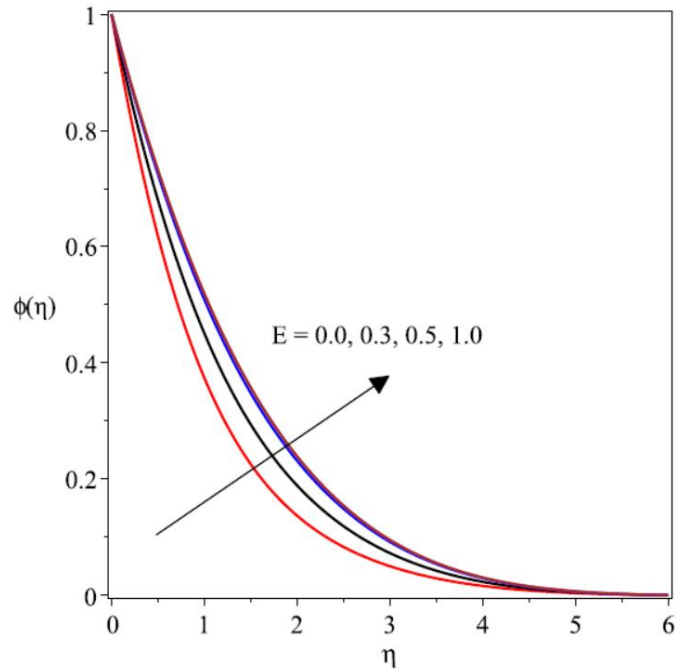
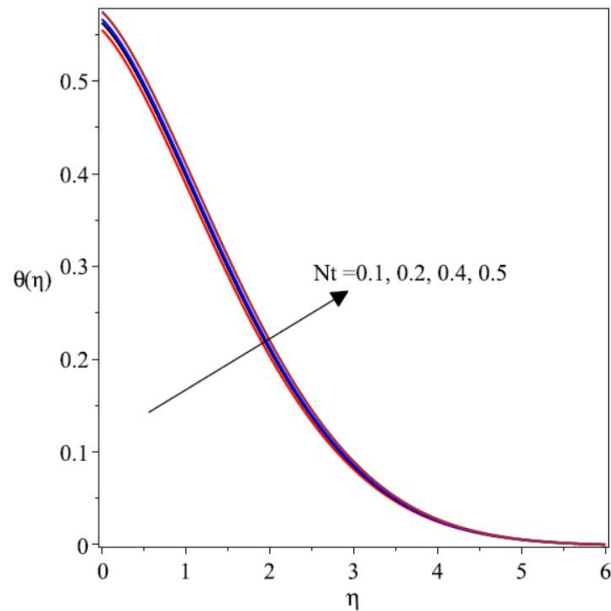

Figure 10 Trend of the concentration due to varying E9

Figure. 11 Trend of the temperature due to varying Nt

However, the concentration field behaves in an opposite manner as it falls significantly in the face of Nb as clearly seen in figure 14. The figure demonstrates that N_b produces a thin layer in the boundary structure and as such causes a decline in the concentration profiles.
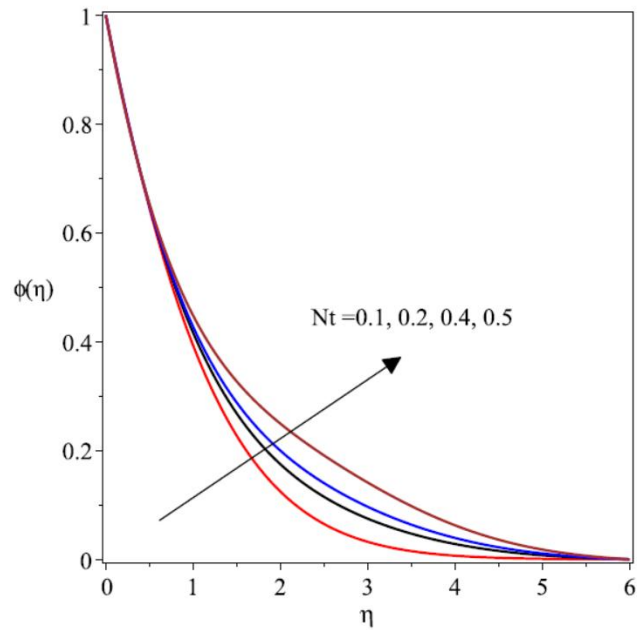
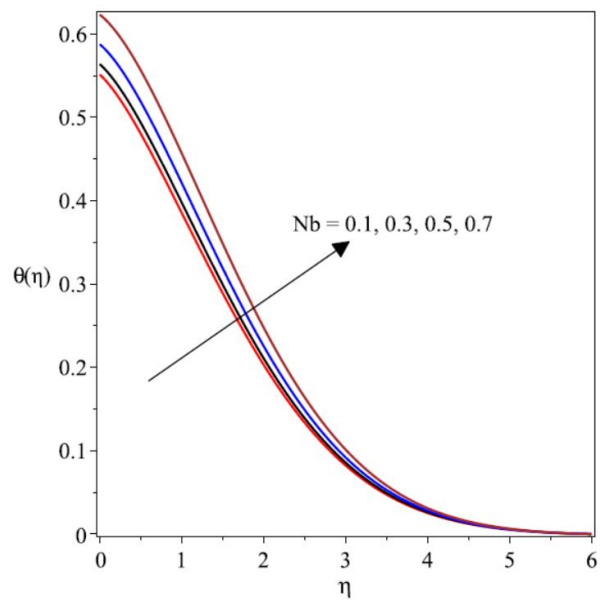Figure. 12 Trend of the concentration due to varying Nt

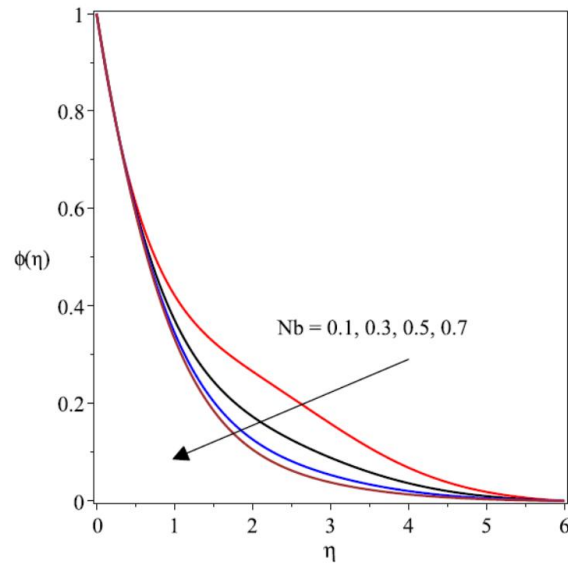Figure. 13 Trend of the concentration due to varying Nb

Figure. 14 Trend of the concentration due to varying Nb

Figure 15 and 16 manifest the behaviour of the mixed convection term on the velocity and thermal profiles. A boost in λ causes the buoyancy force to appreciate over that of viscous force and so, the velocity profiles appreciates, leading to higher fluid flow motion as found in figure 15. On the other hand, thermal bounding surface declines due to growing values of the mixed convection term as depicted in figure 16.
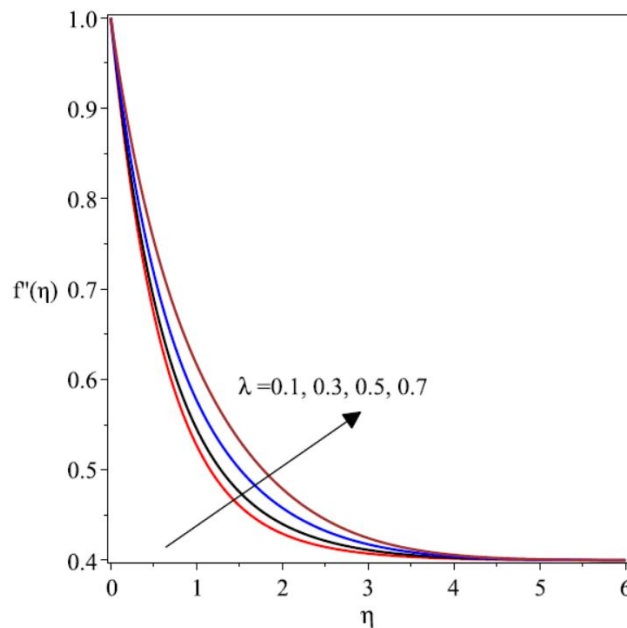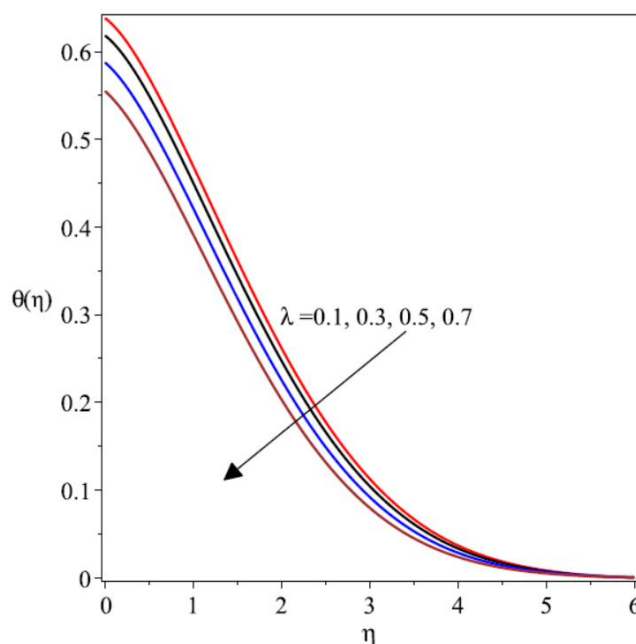

Figure. 15 Trend of the velocity as λ varies

Figure. 16 Trend of the temperature as a result of variations in λ

5. Conclusion

This study investigates the flow of hydromagnetic Williamson nanofluids over a nonlinear stretchable sheet in a material device experiencing non-uniform thermal conductivity. In the heat wall region where convective heat restrictions are present, the effects of viscous dissipation, buoyancy force, mixed convection, thermal radiation, activation energy, and chemical processes have been scrutinised. The major equations have been simplified to ordinary derivatives of order three using a similarity modification method, and then integrated them using the Runge-Kutta Fehlberg algorithm with the shooting approach. Findings are presented in a tabular and graphical format for easy interpretation, and they are highly connected with prior research in the literature. A few key takeaways from this study are as follows:

- The Lorentz force applies a transverse magnetic field to an expanding plate causes the Williamson fluid to experience a significant slowing of its velocity.
- The effects of the Prandtl number dampen the fluid's motion, whereas the Eckert number and mixed convection characteristics cause the fluid's motion to surge.
- In the presence of thermo-migration of small particles and the erratic motion of minute particles in the thermal region, the heat dispersion is much improved as the Eckert number raises the temperature of the fluid.
- As a result of the effects of Sc and γ1, the concentration profiles are shown to decrease, yet the activation energy (E) produces a considerable upward shift in the concentration profiles.

References

[1]. E. O.Fatunmbi, H. A. Ogunseye, P. Sibanda, Magnetohydrodynamic micropolar fluid flow in a porous medium with multiple slip conditions, International Communications in Heat and Mass Transfer 115 (2020) 104577.
[2]. C. Y. Wang. The three dimensional flow due to a stretching flat surface, Phys. Fluids 27, 1915 (1984); doi: 10.1063/1.864868 View online: http://dx.doi.org/10.1063/1.864868
[3]. Hossam A. Nabwey, A. Mahdy, Transient flow of micropolar dusty hybrid nanofluid loaded with Fe3O4-Ag nanoparticles through a porous stretching sheet, Results in Physics 21 (2021) 103777.
[4]. Pal D, Chatterjee S. Heat and mass transfer in MHD non-Darcian flow of a micropolar fluid over a stretching sheet embedded in a porous media with non-uniform heat source and thermal radiation.
[5]. K. Sajjan, K., Shah, N. A., Ahammad, N. A., Raju, C.S.K, Kumar, M. N., Weera, W. Nonlinear Boussinesq and Rosseland approximations on 3D flow in an interruption of Ternary nanoparticles with various shapes of densities and conductivity properties, AIMS Mathematics, 7(10): 1841618449.DOI: 10.3934/math.20221014

[6].   B. Mahanthesh, Mackolil, J.,. Radhika, M., Al-Kouz, W., Siddabasappa. Significance of quadratic thermal radiation and quadratic convection on boundary layer two-phase flow of a dusty nanoliquid past a vertical plate. International Communications in Heat and Mass Transfer, https://doi.org/10.1016/j.icheatmasstransfer.2020.105029

[7].   Qasim, M., Khan, I. and Shafie, S. Heat Transfer in a Micropolar Fluid over a Stretching Sheet with Newtonian Heating,PLoS ONE 8(4) 1-6, (2013).

[8].   Shah, Z., Bonyah, E., Islam, S., Khan, W., Ishaq, M. Radiative MHD thin film flow of Williamson fluid over an unsteady permeable stretching, Heliyon, 4 (2018) e00825. doi: 10.1016/j.heliyon.2018.e00825

[9].   O. Quran, H. Maaitah, H. M Duwairi. Fluid flow and heat transfer characteristics of Williamson fluids flowing in saturated porous media, Advances in Mechanical Engineering (2023). https://doi.org/10.1177/1687813223115715

[10].   Chao, B. T. Jeng, D. R. (1965). Unsteady stagnation point heat transfer. Journal of Heat Transfer 87, 221-230.

[11].   Ibrahim S. M, Suneetha. Effects of heat generation and thermal radiation on steady MHD flow near a stagnation point on a linear stretching sheet in porous medium. Journal of Computational and Applied, Research in Mechanical Engineering. 2015;4:133-144.

[12].   Pandey AK, Kumar M. Effect of viscous dissipation and suction/injection on MHD nanofluid flow over a wedge with porous medium and slip. Alexandria 15 Engineering Journal. 2016;55(4): 31153123.

[13].   Nadeem, S., Hussain, S. T. and Lee, C. Flow of a Williamson fluid over a stretching sheet, Brazilian Journal of Chemical Engineering, 30(3), 615-625 (2013).

[14].   Williamson, R. V. The flow of pseudoplastic materials, Industrial and Engineering Chemistry, 21(11), 1108-1111 (1929).

[15].   Crane, L. J. Flow past a stretching plate. Communicatios Breves, 21, 645-647 (1970).

[16].   Mabood, F. Khan, W.A., Ismail, A.I.M. Approximate analytical modelling of heat and mass transfer in hydromagnetic flow over a non-isothermal stretched surface with heat generation/ absorption and transpiration. Journal of the Taiwan Institute of Chemical Engineers 54 11-19 (2015).

[17].   E.O. Fatunmbi, O. J. Ramonu & S.O. Salawu. Analysis of heat transfer phenomenon in hydromagnetic micropolar nanoliquid over a vertical stretching material featuring convective and isothermal heating conditions, Waves in Random and Complex Media, (2023) DOI: 10.1080/17455030.2023.2173494

[18].   Gupta PS, Gupta AS. Heat and mass transfer on a stretching sheet with suction or blowing. Can. J. Chem. Eng. 1977;55:744-746.

[19].   Mishra SR, Baag S, Mohapatra DK. Chemical reaction and Soret effects on hydromagnetic micropolar fluid along a stretching sheet. Engineering Science and Technology, an Int. Journal. 2016; 19:1919-1928.

[20].   Cortell R. viscous flow and heat transfer over a nonlinearly stretching sheet. Appl Math Comput. 2007;184:864873

[21].   Waqas M, Farooq M, Khan MJ. Magnetohydrodynamic (MHD) mixed convection flow of micropolar liquid due to nonlinear stretched sheet with convective condition. Int J Heat Mass Transfer. 2016;102:766772

[22].   S.U.S. Choi, Enhancing thermal conductivity of fluids with nanoparticles, in: International Mechanical Engineering Congress and Exposition vol. 66, USA, ASME, FED 231/MD, San Francisco, 1995, pp. 99105.

[23].   Mabood F, Yusuf TA, Khan WA. CuAl2O3H2O hybrid nanofluid flow with melting heat transfer, irreversibility analysis and nonlinear thermal radiation. Journal of Thermal Analysis and Calorimetry 2021; 143(2): 973-984.